Published in final edited form as:
J Immunol. 2009 May 1; 182(9): 5268–5275. doi:10.4049/jimmunol.0800681.

Autoantigen Immunization at Different Sites Reveals a Role for Anti-Inflammatory Effects of IFN-γ in Regulating Susceptibility to Experimental Autoimmune Encephalomyelitis[1]

Silvia Pastor[2,3], **Alfredo Minguela**[2,4], **Wentao Mi**, and **E. Sally Ward**[5]
Department of Immunology, University of Texas Southwestern Medical Center, Dallas, TX 75390

Abstract

Experimental autoimmune encephalomyelitis is induced in B10.PL (H-2^u) mice by immunization with the immunodominant N-terminal epitope of myelin basic protein, Ac1-9. In the present study, we show that the site of immunization impacts disease incidence and severity. This effect is more marked in female mice than in males. Although immunization in the flanks is effective in eliciting disease, delivery of Ag in the footpad and tailbase results in poor induction. Analyses of the immune responses in female mice following different immunization regimens indicates that resistance to disease is accompanied by higher levels of IFN-γ and $CD11b^+Gr\text{-}1^{int}$ myeloid cells. Such myeloid cells are known to have a suppressive function, and consistent with this knowledge, blockade of IFN-γ results in increased disease activity and decreased levels of splenic $CD11b^+Gr\text{-}1^{int}$ cells. Conversely, injection of adjuvants (CFA or Pam_3CSK_4) in the footpad decreases experimental autoimmune encephalomyelitis incidence and severity. Our study indicates that the site of immunization can impact the magnitude of the ensuing inflammatory response, and that at a certain threshold a protective, regulatory circuit can be elicited.

Murine experimental autoimmune encephalomyelitis (EAE)[6] is taken to be a representative model of multiple sclerosis (1). In H-2^u mice, $CD4^+$ T cells that recognize the immunodominant N-terminal epitope of myelin basic protein (MBP) acetylated at the N terminus (Ac1-9) associated with the MHC class II molecule, I-A^u, play a central role in the disease process (2). Disease is initiated by entry of autoreactive T cells into the CNS, followed by the influx of macrophages and the activation of resident cells such as microglial cells (3,4). This inflammatory environment results in CNS destruction involving demyelination that in turn causes ascending paralysis.

A limitation toward understanding the triggers of autoimmunity has, until recently, been the lack of available tools such as appropriate peptide-MHC multimers and sensitive ELISpot

[1]This work was supported by Grant R01 AI/NS 42949 from the National Institutes of Health and Grant RG 2411 from the National Multiple Sclerosis Society. A.M. was supported by a Fellowship BAE 00/5030 and 01/5037 from the Fondo de Investigacion Sanitaria. CIBEREHD is funded by the Instituto de Salud Carlos III.

[5]Address correspondence and reprint requests to Dr. E. Sally Ward, Department of Immunology, University of Texas Southwestern Medical Center, 6000 Harry Hines Boulevard, Dallas, TX 75390-9093. sally.ward@utsouthwestern.edu .
[2]S.P. and A.M. contributed equally to this work.
[3]Current address: Ophthalmology Institute of Alicante (Vissum Corporation), Avda. Denia s/n, Edificio Vissum, Alicante, Spain.
[4]Current address: Immunology Service, University Hospital “Virgen de la Arrixaca”, El Palmar, Murcia, Centro de Investigación Biomédica en Red de Enfermedades Hepáticas y Digestivas (CIBEREHD o Ciberehd), Spain.

Disclosures
The authors have no financial conflict of interest.

[6]Abbreviations used in this paper: EAE, experimental autoimmune encephalomyelitis; MBP, myelin basic protein; LN, lymph node.

assays to quantitatively assess autoreactive T cell responses (5–8). As a result, factors such as the impact of gender on quantitative aspects of pathogenic T cell responses are poorly understood. We have developed the use of MBP1-9:I-A^u multimers to detect Ag-specific T cells in the B10.PL mouse model of EAE (5,9) and are using these to gain insight into the processes that lead to autoimmunity.

In the current study we have analyzed the effect of immunization site (footpad and tailbase or flank) on the incidence and severity of disease in B10.PL mice. We observe that the site of immunization with the MBP epitope, Ac1-9, can impact EAE severity and incidence, with flank immunization inducing greater disease activity relative to delivery of Ag in the footpad and tailbase. This difference is more marked in female mice relative to male mice, and is consistent with earlier studies in B10.PL mice in which the disease susceptibility of female mice was lower (10). To investigate the mechanistic basis for the differences in disease activity, we have used MBP1-9:I-A^u multimers (5) to enumerate and characterize autoantigen-specific T cell responses following immunization. We show that the immunization site affects the magnitude of the T cell response in female mice, with higher levels of Ag-specific T cells in the spleens correlating with disease resistance. The higher T cell responses are accompanied by increased levels of IFN-γ and $CD11b^+Gr\text{-}1^{int}$ myeloid suppressor cells (MSCs) that have been demonstrated to have suppressive activity in murine models of cancer, autoimmunity and infectious disease (11–15). The anti-inflammatory effects that we observe can be reversed or enhanced by delivery of anti-IFN-γ Ab or adjuvants, respectively. Consistent with the IFN-γ dependence of MSCs, a lower number of these cells was observed in spleens of mice treated with anti-IFN-γ Ab. Our analyses have relevance to understanding the factors that regulate pathogenic T cell responses in murine EAE.

Materials and Methods

Reagents and cell lines

The N-terminal-acetylated peptide of MBP (Ac1-9, ASQKRPSQR) was purchased from CS Bio. The TLR2 antagonist lipopeptide, Pam_3CSK_4, was purchased from EMC Microcollections.

The following fluorescently labeled Abs were used for flow cytometry and purchased from BD Biosciences: FITC-, PerCP-, and allophycocyanin-labeled anti-CD4 (L3T4), PerCP-labeled anti-CD45 (30-F11), FITC-labeled and purified anti-TCR Vα2 (B20.1), allophycocyanin-labeled anti-IFN-γ (XMG1.2), PE-labeled anti-TNF-α (MP6-XT22), PE-labeled anti-IL-17 (TC11-18H10), PerCP- and PE-labeled anti-Gr-1 (RB6-8C5), allophycocyanin-labeled anti-CD11b (M1/70) and allophycocyanin-labeled anti-BrdU. FITC-labeled anti-BrdU was obtained from Invitrogen. PE-labeled anti-F4/80 was purchased from eBioscience. Anti-I-A^u Ab was purified from the 10.2.16 hybridoma (16) and labeled with FITC using standard methods.

Hybridomas expressing anti-IFN-γ Ab (R4-6A2, rat IgG1) and a rat IgG1 isotype control (CRL-1912) were purchased from the American Type Culture Collection. They were expanded in culture medium containing FCS depleted of bovine IgG by passage over protein G-Sepharose. IgGs were purified from culture supernatants using protein G-Sepharose. For use in some experiments, anti-IFN-γ Ab (R4-6A2) was purchased from BD Biosciences or eBioscience.

Recombinant peptide-MHC multimers

To detect Ac1-9:I-A^u-specific $CD4^+$ T cells, biotinylated MBP1-9[4Y]:I-A^u multimeric complexes (tetramers) were generated and purified as previously described (5,9). For detection,

tetrameric complexes were prepared by incubating sites specifically biotinylated MBP1-9 [4Y]:I-A^u with PE-labeled Extravidin (Sigma-Aldrich) in an optimized molar ratio for 10–30 min at 4°C (5). The peptide-I-A^u complexes were made using a higher affinity analog of MBP, MBP1-9[4Y] (17–19) because multimers containing the wild-type MBP1-9 epitope are unstable (5). The position 4 substitution of lysine by tyrosine (4Y) has been shown to not affect the qualitative nature of T cell recognition (17,20,21).

Mice

B10.PL (H-2^u) male and female mice were purchased from The Jackson Laboratory. Transgenic male and female mice expressing the β-chain of the 172.10 TCR (22,23), backcrossed onto the B10.PL background, were provided by Dr. J. Goverman (University of Washington, Seattle, WA). Mice were bred and maintained in a specific pathogen-free environment at the University of Texas Southwestern Medical Center animal facility in compliance with institutional guidelines. All mice were 6 to 10 wk of age when experiments were initiated.

Induction of EAE

For induction of EAE, male and female B10.PL mice were s.c. immunized with 200 μg of the N-terminal-acetylated epitope of MBP, Ac1-9, in one footpad and the tailbase (50 μl at each site, footpad/tailbase immunization) or at two or four sites in the flanks (25 or 50 μl at each site, flank immunization). Peptide was emulsified in CFA (Sigma-Aldrich) supplemented with 4 mg/ml *Mycobacterium tuberculosis* (Difco). For delivery of the lipopeptide adjuvant, Pam_3CSK_4 was emulsified in IFA at a concentration of 500 μg/ml (Sigma-Aldrich) and s.c. injected only in one footpad (50 μl) of mice previously immunized with Ac1-9/CFA in the flanks. For delivery of CFA or IFA without peptide, adjuvants were diluted with an equal volume of PBS and emulsified. Mice were injected with 50 μl of each emulsion in the footpad following immunization with Ac1-9/CFA in the flanks. Pertussis toxin (200 ng/mouse; List Biological Laboratories) in PBS was i.p. injected at the time of immunization and 48 h later.

EAE evaluation was performed as described (24): 0, no paralysis; 1, limp tail; 2, moderate hind limb weakness; 3, severe hind limb weakness; 4, complete hind limb paralysis; 5, quadriplegia; and 6, death due to disease. Clinical signs of EAE were assessed for up to 30 days after immunization. Mean clinical scores were derived from scores for all mice within each group and include disease-free mice. Mice that showed an EAE score of 4 for longer than 5 days or a score of 5 were sacrificed for ethical reasons and in accordance with institutional guidelines.

Treatment of mice with anti-IFN-γ Ab

Female B10.PL mice immunized with 200 μg Ac1-9 in the footpad and tailbase, as described above, were treated with 100 μg of anti-IFN-γ Ab (rat IgG1, R4-6A2) injected through the tail vein on days 6 and 9 after immunization. As a control, 100 μg of an irrelevant rat IgG1 Ab was used. Female B10.PL mice immunized in the flanks with 200 μg Ac1-9, as described above, were used as a control for EAE induction. In some experiments, mice were sacrificed at different time points following immunization and $CD11b^+Gr\text{-}1^+$ populations analyzed by flow cytometry.

Flow cytometric analyses

For CNS analyses of immunized mice, animals were anesthetized and perfused through the right ventricle with 10 ml of ice-cold PBS containing 2 mM EDTA disodium salt. Spleens, lymph nodes (LNs), and CNS (brain and spinal cord) samples were subsequently harvested into cold RPMI 1640 (Invitrogen) containing 2 mM EDTA disodium salt. Cell suspensions were obtained by passing tissues through a thin wire mesh. CNS suspensions were pulsed at

1000 rpm to discard debris and then treated as for the cell suspensions from the other tissues. Suspensions were depleted of RBCs using ammonium chloride buffer and then washed twice with cold PBS.

For flow cytometric analyses, all cell suspensions were treated with Fc block (CD16/CD32 Abs; BD Biosciences) for 10 min before staining with the appropriate combinations of fluorescent Abs at 4°C and then washed using standard methods. To detect Ag-specific $CD4^+$ T cells in LNs, spleens, and CNS samples, cells were incubated with PE-labeled MBP1-9 [4Y]:I-A^u multimers together with other fluorescently labeled Abs (as indicated in the figure legends) at 12°C for 2 h and washed twice. When staining for Vα2 expression was conducted, cells were incubated with multimers and other Abs before washing and incubation with the anti-Vα2 Ab. Labeled cells were acquired using a FACSCalibur (BD Biosciences) and analyzed using the software (FlowJo Tree Star) or WinMDI 2.8 (Scripps Research Institute, http://facs.scripps.edu). Cell counts of each subpopulation were estimated by adding 2×10^4 propidium iodide-labeled BW5147 cells to each tube before flow cytometric analysis, and cell numbers were determined for each sample as previously described (25). Macrophage populations were demarcated based on forward scatter vs side scatter and CD45 expression vs side scatter as described (9).

In vivo proliferation analysis by BrdU staining

Four hours before harvesting tissues, all mice were i.p. injected twice at 2-h intervals with 500 μg of BrdU (BD Biosciences). Mice were sacrificed 2 h after the last BrdU injection. Single cell suspensions of LNs and spleens were obtained as described above and stained with PerCP-labeled anti-CD4. Labeled cells were then washed, fixed, permeabilized and treated with DNase at 37°C for 60 min to expose DNA. Cells were washed and stained with FITC-or allophycocyanin-labeled anti-BrdU Abs at room temperature for 20 min and finally washed and analyzed by flow cytometry as above.

In vitro activation assays

Spleen cells (3×10^5/well) were cultured in 96-well plates in complete DMEM containing 2 mM L-glutamine, 5×10^{-5} M 2-ME, 1 mM sodium pyruvate, 100 U/ml penicillin, 100 μg/ml streptomycin (Invitrogen), and 10% FCS. Ac1-9 peptide was added at different concentrations as indicated in the figure legends. Following 3 days of stimulation, IFN-γ levels in culture supernatants were determined by ELISA as previously described (26) and expressed as mean ± SE of triplicate wells. Proliferation following 96 h of culture was analyzed by adding 1 μCi of [^{3}H]thymidine (Amersham Biosciences) to each well for the last 16 h, and was expressed as [^{3}H]thymidine incorporation (mean cpm ± SE of triplicate wells).

Intracellular cytokine detection

Splenocytes were harvested as described above from mice immunized at distinct injection sites with 200 μg of Ac1-9 at different time points following immunization. Splenocytes (2×10^6/well in 48-well plates) were stimulated with 50 μg/ml Ac1-9 in complete DMEM for 4 h at 37°C in a 5% CO_2 incubator. For each experimental condition, four to six wells were used. A total of 1 μl of Golgi Plug containing brefeldin A (BD Biosciences) was added to the cultures. Cells were then pooled for each condition, washed twice with PBS, and fixed with 5% formalin at room temperature for 20 min. Cells were then washed once with PBS, once with 1% BSA/PBS, and permeabilized with 0.1% saponin in 1% BSA/PBS at room temperature for 10 min. Cells were stained with FITC- or Alexa Fluor 488-labeled anti-CD4, allophycocyanin-labeled anti-IFN-γ, and PE-labeled anti-IL-17, or allophycocyanin-labeled anti-CD4 and PE-labeled anti-TNF-α, washed and analyzed by flow cytometry as described above.

Statistical analyses

For statistical analyses, SPSS software was used. Normal distribution of experimental data was tested using Kolmogorv-Sminorff test. The Kruskal-Wallis nonparametric test was used to compare all experimental groups and when significant differences were found, the Mann-Whitney *U* test was used for pairwise comparisons. In all cases, values of $p \leq 0.05$ were considered to indicate significant differences.

Results

Immunization at different body sites affects EAE incidence and severity

Male or female B10.PL mice were immunized in the footpad and tailbase or flanks with 200 μg of the N-terminal-acetylated epitope of MBP, Ac1-9. Disease incidence and severity were monitored. Significantly lower disease activity was seen in female mice following footpad/tailbase immunization relative to flank immunization (Fig. 1, *top*). By contrast, although immunization in the flanks appeared to result in higher disease activity with a more chronic course relative to footpad/tailbase immunization in male mice, the incidence was the same and the differences in mean clinical score were not significant (Fig. 1). In addition, immunization at either two or four sites in the flanks was more effective in inducing disease relative to footpad/tailbase delivery in female mice (Fig. 1 and data not shown), indicating that the difference in disease is due to variations in delivery site rather than the number of immunization sites used.

The site of immunization affects adaptive and innate immune responses

We investigated the possible mechanistic basis for the difference in disease incidence and severity in female mice following immunization at different sites. The analysis of Ag-specific tetramer-positive $CD4^+$ ($CD4^+tet^+$) T cells using MBP1-9[4Y]:I-A^u multimers (5,9), and proliferating $CD4^+$ T cells, in spleens and pooled LNs indicated differences for cells isolated from female mice immunized in the footpad/tailbase or flanks (Fig. 2*A*). Higher percentages of Ag-specific and proliferating cells were observed in the spleens and pooled LNs of mice immunized in the footpad/tailbase relative to the flanks, and these differences were most marked at day 10 following immunization (Fig. 2*A*). EAE is characterized by an inflammatory infiltrate in the CNS comprising (Ag-specific) $CD4^+$ T cells, macrophages and granulocytes (4,27,28). Consistent with the higher disease activity, more infiltrating $CD4^+$ T cells and macrophages were observed in the CNS of female mice that had been immunized in the flanks relative to those immunized in the footpad/tailbase (Fig. 2*A*). We also assessed cytokine production following immunization of female mice at different sites. The greater percentage of Ag-specific T cells in the spleen of female mice immunized in the footpad/tailbase was accompanied by a higher level of inflammatory cytokine production (IFN-γ and TNF-α) (Fig. 2*B*). Because IFN-γ has been shown to down-regulate the number of Th17 (IL-17-producing) cells (29–32), we also analyzed the production of this cytokine. Again, however, higher levels were observed in female mice following footpad/tailbase immunization, indicating that the elevated levels of IFN-γ do not appear to suppress the in vivo expansion of Th17 cells.

Similar T cell responses in male and female mice following footpad/tailbase immunization

Because male mice appeared to be more susceptible to EAE relative to females following footpad/tailbase immunization (Fig. 1), we compared immune responses across gender following immunization at these sites. This gender difference in disease susceptibility was also observed in B10.PL mice that transgenically express the β-chain of the 172.10 TCR mice (23) (Vβ172.10 mice) that is specific for Ac1-9 complexed with I-A^u (Fig. 3*A*). The higher number of Ag-specific T cells in these transgenic mice facilitates their quantitation. Analyses of Ag-specific $CD4^+$ T cells using MBP1-9[4Y]:I-A^u tetramers (5,9) at day 11 (B10.PL mice) or day 4 (Vβ172.10 mice) postimmunization indicated that the percentages of such cells were

similar in the spleen and pooled LNs in male and female mice (Fig. 3*B*). The ratio values of $V\alpha2^+$ to $V\alpha2^-$ tetramer-positive cells were analogous, indicating that the T cell repertoires were similar. Analysis of the absolute numbers of tetramer-positive cells at day 11 (B10.PL mice) and day 4 (Vβ172.10 mice) also indicated that, consistent with the data shown in Fig. 3*B*, there were not major differences across gender (Fig. 3*C*). However, by day 18 (B10.PL mice) or day 11 (Vβ172.10 mice) postimmunization, the number of Ag-specific T cells in both LNs and spleens of female mice was higher, possibly because these cells had not infiltrated into the CNS.

Consistent with the higher disease incidence and severity in male mice, the number of $CD4^+tet^+$ T cells and macrophages infiltrating the CNS were substantially higher in male mice relative to female mice at times around the peak of overt disease (day 18 for B10.PL mice, day 11 for Vβ172.10 mice postimmunization) (Fig. 3*C*). However, analysis of the in vitro recall responses of cells isolated 11 days postimmunization indicated similar proliferation and IFN-γ production in male and female mice (Fig. 3*D*). The difference in disease incidence and severity between male and female mice following footpad/tailbase immunization is therefore not due to variations in peripheral Ag-specific T cell numbers or their responsiveness. Consequently, we decided to focus our subsequent analyses on female mice following immunization at distinct sites because this focus resulted in clear differences in T cell responses (Fig. 2).

The site of immunization affects the number of $CD11b^+Gr\text{-}1^+$ myeloid cells

$CD11b^+Gr\text{-}1^+$ (MSCs) have recently been shown to have potent antiinflammatory effects in different models of inflammation (11–15). Specifically, the $Gr\text{-}1^+$ cells can be divided into two subpopulations, $Gr\text{-}1^{high}$ and $Gr\text{-}1^{int}$, of which the $Gr\text{-}1^{int}$ subset have more potent suppressive activity in EAE (14). The number of these cells increase markedly in the spleens of female mice following injection with emulsified CFA (without peptide) (14) (Fig. 4*A*). We therefore analyzed these cell subsets in the spleens of mice that had been immunized with Ac1-9 (in CFA) at distinct sites (Fig. 4, *B* and *C*). Correlating with the induction of a higher number of Ag-specific T cells, we observed a higher number of myeloid cells in the spleens in female mice immunized in the footpad/tailbase relative to the flanks (Fig. 4*C*). These differences were particularly marked for the $CD11b^+Gr\text{-}1^{int}$ population and became apparent from day 10 postimmunization onward. Taken together, the dependence of MSCs on IFN-γ (12–14,33) combined with the higher level of IFN-γ-producing $CD4^+$ T cells in spleens of females immunized in the footpad/tailbase might therefore contribute to a regulatory circuit that results in lower disease incidence. Conversely, in flank-immunized female mice, a combination of the lower number of both splenic myeloid cells and IFN-γ-producing $CD4^+$ T cells might predispose mice toward disease.

IFN-γ blockade exacerbates EAE incidence and severity and results in a decrease in the number of splenic $CD11b^+Gr\text{-}1^{int}$ cells

The dependence of MSCs on IFN-γ in both EAE and other disease models (12–14,33) prompted us to assess whether reduction of IFN-γ levels in vivo might lead to enhanced susceptibility to disease. Female mice were therefore immunized in the footpad/tailbase or flanks and treated with anti-IFN-γ Ab or isotype control. IFN-γ blockade resulted in disease incidence and severity in footpad/tailbase-immunized mice that was analogous to that seen in flank-immunized, female mice (Fig. 5*A*). Importantly, analysis of $CD11b^+Gr1^{int}$ cell number following anti-IFN-γ treatment indicated that IFN-γ blockade resulted in a reduced number of MSCs on days 13 and 15 postimmunization, which in turn correlates with increased disease susceptibility (Fig. 5*B*).

Adjuvant delivery in the footpad protects against EAE

Because CFA is a potent inducer of MSCs (14) as shown (Fig. 4*A*), we also analyzed whether the induction of inflammatory responses via delivery of CFA or other potent TLR agonists such as Pam_3CSK_4 (in IFA), in the footpad would prevent disease development in female mice. Female mice were immunized with Ac1-9 in the flanks and with adjuvant only in the footpad. This regimen resulted in inhibition of disease for both adjuvants (Fig. 5*C*) that was not seen when IFA was used. Thus, the delivery of adjuvants such as CFA or Pam_3CSK_4 without Ag in the footpad results in protection against disease induction, consistent with the concept that this innate stimulation results in an anti-inflammatory feedback loop.

Discussion

The current study provides insight into the factors that lead to overt EAE in B10.PL mice. We observe that female mice are more resistant to the induction of EAE when they are immunized in the footpad/tailbase relative to the flanks, but that the effect of immunization site is less marked in male mice. For female mice immunized at distinct sites, our data show that relative to flank immunization, footpad/tailbase immunization results in a higher number of Ag-specific T cells in spleens and pooled LNs that paradoxically lead to increased disease resistance. These observations are reminiscent of our earlier studies in which we reported that immunization of mice with high effective doses of autoantigen (MBP1-9[4Y]) induce an increased level of Ag-specific T cells, resulting in an antiinflammatory feedback loop involving IFN-γ (9).

Significantly, we demonstrate that higher levels of IFN-γ producing cells and $CD11b^+Gr\text{-}1^+$ myeloid cells are induced in the spleens of female mice following footpad/tailbase immunization relative to flank immunization. IFN-γ is known to have both proinflammatory and anti-inflammatory effects (34,35). The ability of IFN-γ to induce NO production by myeloid cells such as macrophages and neutrophils is well documented (11,13,36–38). Recent studies have also shown that the monocytic subset of $CD11b^+Gr\text{-}1^{int}$ cells are involved in mediating anti-inflammatory effects in murine EAE (14). Furthermore, this suppression is dependent on IFN-γ production by $CD4^+$ T cells. Consistent with these observations, when the $CD11b^+Gr\text{-}1^{high}$ and $CD11b^+Gr\text{-}1^{int}$ populations of myeloid cells are compared following footpad/tailbase vs flank immunization of female mice, more marked increases in the $CD11b^+Gr\text{-}1^{int}$ population in footpad/tailbase-immunized mice are seen. In addition, footpad/tailbase immunization combined with IFN-γ blockade results in exacerbation of disease incidence and severity, combined with decreased levels of $CD11b^+Gr\text{-}1^{int}$ cells. These observations are congruent with the IFN-γ dependence of these suppressor cells. Conversely, delivery of adjuvants (CFA, Pam_3CSK_4) in the footpad/tailbase combined with Ag immunization in the flanks of female mice protects against disease. Such adjuvants are known to act through TLR2/4 (CFA) and TLR1/2 (Pam_3CSK_4), and as such can elicit potent innate stimulation of myeloid cells (Refs. 39 and 40, and this study).

Alternative mechanisms for the anti-inflammatory effects of IFN-γ have also been described that include the inhibition of the development of IL-17-producing cells (29–32) or the induction of CD3ζ down-regulation via a mechanism that involves MSCs (41,42). Our data do not support a role for IFN-γ regulatory effects on Th17 cells because IL-17-producing cell numbers are higher in female mice following Ag delivery via footpad/tailbase relative to flanks. Furthermore, we do not observe T cell hyporesponsiveness in mice that are protected against disease, indicating that CD3ζ down-regulation does not occur.

The factors that lead to the gender differences following immunization in the footpad and tailbase of male and female mice remain enigmatic, although our data allow for the exclusion of several possible mechanisms. First, comparison of immunized male and female mice indicates that there is no major difference in either Ag-specific T cell numbers or Ag

responsiveness across genders. In addition, we observe a similar number of $CD11b^{+}Gr1^{int}$ cells in male and female mice following immunization (data not shown). Second, our in vitro restimulation data in which we do not see differences in responsiveness of splenic cells from male vs female mice indicate that gender-specific variations in regulatory T cells (43) or other regulatory cells in male and female B10.PL mice cannot account for the differences in disease susceptibility. Furthermore, a recent study has shown that regulatory T cells do not control autoimmunity in the inflamed CNS in EAE (44), although other studies have suggested that regulatory T cells expand in the CNS concomitant with the resolution of disease (45). Based on our comparative studies of male and female mice, our data would, however, be congruent with the possibility that the difference in disease susceptibility is due to gender variation in blood-brain barrier permeability, which in turn could be hormonally regulated (46,47). In this context, the gender difference in disease susceptibility is observed for Vβ172.10 mice in which EAE can be induced in the absence of pertussis toxin, consistent with earlier observations indicating that variations in the effects of pertussis toxin across gender cannot fully account for increased disease activity in male B10.PL mice (10). In addition, it is possible that female hormones are conducive to the anti-inflammatory effects of MSCs.

In conclusion, our observations indicate a role for antiinflammatory effects of IFN-γ-dependent MSCs that manifest their protective effects following immunization in the footpad and tail-base, but not in flanks, of female B10.PL mice. These studies have relevance to understanding the regulatory mechanisms that lead to EAE, in addition to suggesting that the modulation of MSCs might provide a therapeutic option.

References

1. Brown A, McFarlin DE, Raine CS. Chronologic neuropathology of relapsing experimental allergic encephalomyelitis in the mouse. Lab. Invest 1982;46:171–185. [PubMed: 7062721]
2. Zamvil SS, Mitchell DJ, Moore AC, Kitamura K, Steinman L, Rothbard JB. T-cell epitope of the autoantigen myelin basic protein that induces encephalomyelitis. Nature 1986;324:258–260. [PubMed: 2431317]
3. Steinman L, Martin R, Bernard C, Conlon P, Oksenberg JR. Multiple sclerosis: deeper understanding of its pathogenesis reveals new targets for therapy. Annu. Rev. Neurosci 2002;25:491–505. [PubMed: 12052918]
4. Elhofy A, Kennedy KJ, Fife BT, Karpus WJ. Regulation of experimental autoimmune encephalomyelitis by chemokines and chemokine receptors. Immunol. Res 2002;25:167–175. [PubMed: 11999170]
5. Radu CG, Anderton SM, Firan M, Wraith DC, Ward ES. Detection of autoreactive T cells in $H\text{-}2^{u}$ mice using peptide-MHC multimers. Int. Immunol 2000;12:1553–1560. [PubMed: 11058575]
6. Reddy J, Bettelli E, Nicholson L, Waldner H, Jang MH, Wucherpfennig KW, Kuchroo VK. Detection of autoreactive myelin proteolipid protein 139–151-specific T cells by using MHC II (IAs) tetramers. J. Immunol 2003;170:870–877. [PubMed: 12517952]
7. Targoni OS, Baus J, Hofstetter HH, Hesse MD, Karulin AY, Boehm BO, Forsthuber TG, Lehmann PV. Frequencies of neuroantigen-specific T cells in the central nervous system versus the immune periphery during the course of experimental allergic encephalomyelitis. J. Immunol 2001;166:4757–4764. [PubMed: 11254738]
8. Hofstetter HH, Targoni OS, Karulin AY, Forsthuber TG, Tary-Lehmann M, Lehmann PV. Does the frequency and avidity spectrum of the neuroantigen-specific T cells in the blood mirror the autoimmune process in the central nervous system of mice undergoing experimental allergic encephalomyelitis? J. Immunol 2005;174:4598–4605. [PubMed: 15814682]
9. Minguela A, Pastor S, Mi W, Richardson JA, Ward ES. Feedback regulation of murine autoimmunity via dominant anti-inflammatory effects of interferon γ. J. Immunol 2007;178:134–144. [PubMed: 17182548]

10. Papenfuss TL, Rogers CJ, Gienapp I, Yurrita M, McClain M, Damico N, Valo J, Song F, Whitacre CC. Sex differences in experimental autoimmune encephalomyelitis in multiple murine strains. J. Neuroimmunol 2004;150:59–69. [PubMed: 15081249]
11. Mazzoni A, Bronte V, Visintin A, Spitzer JH, Apolloni E, Serafini P, Zanovello P, Segal DM. Myeloid suppressor lines inhibit T cell responses by an NO-dependent mechanism. J. Immunol 2002;168:689–695. [PubMed: 11777962]
12. Kusmartsev SA, Li Y, Chen SH. Gr-1^{+} myeloid cells derived from tumor-bearing mice inhibit primary T cell activation induced through CD3/CD28 costimulation. J. Immunol 2000;165:779–785. [PubMed: 10878351]
13. Zehntner SP, Brickman C, Bourbonniere L, Remington L, Caruso M, Owens T. Neutrophils that infiltrate the central nervous system regulate T cell responses. J. Immunol 2005;174:5124–5131. [PubMed: 15814744]
14. Zhu B, Bando Y, Xiao S, Yang K, Anderson AC, Kuchroo VK, Khoury SJ. CD11b^{+}Ly-6C^{hi} suppressive monocytes in experimental autoimmune encephalomyelitis. J. Immunol 2007;179:5228–5237. [PubMed: 17911608]
15. Serafini P, Borrello I, Bronte V. Myeloid suppressor cells in cancer: recruitment, phenotype, properties, and mechanisms of immune suppression. Semin. Cancer Biol 2006;16:53–65. [PubMed: 16168663]
16. Oi VT, Jones PP, Goding JW, Herzenberg LA. Properties of monoclonal antibodies to mouse Ig allotypes, H-2, and Ia antigens. Curr. Top. Microbiol. Immunol 1978;81:115–120. [PubMed: 567555]
17. Fairchild PJ, Wildgoose R, Atherton E, Webb S, Wraith DC. An autoantigenic T cell epitope forms unstable complexes with class II MHC: a novel route for escape from tolerance induction. Int. Immunol 1993;5:1151–1158. [PubMed: 7694643]
18. Mason K, Denney DWJ, McConnell HM. Myelin basic protein peptide complexes with the class II MHC molecules I-A^{u} and I-A^{k} form and dissociate rapidly at neutral pH. J. Immunol 1995;154:5216–5227. [PubMed: 7537302]
19. Fugger L, Liang J, Gautam A, Rothbard JB, McDevitt HO. Quantitative analysis of peptides from myelin basic protein binding to the MHC class II protein, I-A^{u}, which confers susceptibility to experimental allergic encephalomyelitis. Mol. Med 1996;2:181–188. [PubMed: 8726461]
20. Anderton SM, Radu CG, Lowrey PA, Ward ES, Wraith DC. Negative selection during the peripheral immune response to antigen. J. Exp. Med 2001;193:1–11. [PubMed: 11136816]
21. Huang JC, Han M, Minguela A, Pastor S, Qadri A, Ward ES. T cell recognition of distinct peptide:I-A^{u} conformers in murine experimental autoimmune encephalomyelitis. J. Immunol 2003;171:2467–2477. [PubMed: 12928395]
22. Urban JL, Kumar V, Kono DH, Gomez C, Horvath SJ, Clayton J, Ando DG, Sercarz EE, Hood L. Restricted use of T cell receptor V genes in murine autoimmune encephalomyelitis raises possibilities for antibody therapy. Cell 1988;54:577–592. [PubMed: 2456857]
23. Goverman J, Woods A, Larson L, Weiner LP, Hood L, Zaller DM. Transgenic mice that express a myelin basic protein-specific T cell receptor develop spontaneous autoimmunity. Cell 1993;72:551–560. [PubMed: 7679952]
24. Critchfield JM, Racke MK, Zuniga-Pflucker JC, Cannella B, Raine CS, Goverman J, Lenardo MJ. T cell deletion in high antigen dose therapy of autoimmune encephalomyelitis. Science 1994;263:1139–1143. [PubMed: 7509084]
25. Marin L, Minguela A, Torio A, Moya-Quiles MR, Muro M, Montes-Ares O, Parrado A, Alvarez-Lopez DM, Garcia-Alonso AM. Flow cytometric quantification of apoptosis and proliferation in mixed lymphocyte culture. Cytometry A 2003;51:107–118. [PubMed: 12541285]
26. Deng C, Minguela A, Hussain RZ, Lovett-Racke AE, Radu C, Ward ES, Racke MK. Expression of the tyrosine phosphatase SRC homology 2 domain-containing protein tyrosine phosphatase 1 determines T cell activation threshold and severity of experimental autoimmune encephalomyelitis. J. Immunol 2002;168:4511–4518. [PubMed: 11970996]
27. Juedes AE, Hjelmstrom P, Bergman CM, Neild AL, Ruddle NH. Kinetics and cellular origin of cytokines in the central nervous system: insight into mechanisms of myelin oligodendrocyte glycoprotein-induced experimental autoimmune encephalomyelitis. J. Immunol 2000;164:419–426. [PubMed: 10605038]

28. Kawakami N, Nagerl UV, Odoardi F, Bonhoeffer T, Wekerle H, Flu¨gel A. Live imaging of effector cell trafficking and autoantigen recognition within the unfolding autoimmune encephalomyelitis lesion. J. Exp. Med 2005;201:1805–1814. [PubMed: 15939794]
29. Murphy CA, Langrish CL, Chen Y, Blumenschein W, McClanahan T, Kastelein RA, Sedgwick JD, Cua DJ. Divergent pro- and antiinflammatory roles for IL-23 and IL-12 in joint autoimmune inflammation. J. Exp. Med 2003;198:1951–1957. [PubMed: 14662908]
30. Langrish CL, Chen Y, Blumenschein WM, Mattson J, Basham B, Sedgwick JD, McClanahan T, Kastelein RA, Cua DJ. IL-23 drives a pathogenic T cell population that induces autoimmune inflammation. J. Exp. Med 2005;201:233–240. [PubMed: 15657292]
31. Harrington LE, Hatton RD, Mangan PR, Turner H, Murphy TL, Murphy KM, Weaver CT. Interleukin 17-producing $CD4^+$ effector T cells develop via a lineage distinct from the T helper type 1 and 2 lineages. Nat. Immunol 2005;6:1123–1132. [PubMed: 16200070]
32. Park H, Li Z, Yang XO, Chang SH, Nurieva R, Wang YH, Wang Y, Hood L, Zhu Z, Tian Q, Dong C. A distinct lineage of CD4 T cells regulates tissue inflammation by producing interleukin 17. Nat. Immunol 2005;6:1133–1141. [PubMed: 16200068]
33. Atochina O, Daly-Engel T, Piskorska D, McGuire E, Harn DA. A schistosome-expressed immunomodulatory glycoconjugate expands peritoneal $Gr1^+$ macrophages that suppress naive $CD4^+$ T cell proliferation via an IFN-γ and nitric oxide-dependent mechanism. J. Immunol 2001;167:4293–4302. [PubMed: 11591752]
34. Muhl H, Pfeilschifter J. Anti-inflammatory properties of pro-inflammatory interferon-γ. Int. Immunopharmacol 2003;3:1247–1255. [PubMed: 12890422]
35. Willenborg DO, Staykova M, Fordham S, O'Brien N, Linares D. The contribution of nitric oxide and interferon γ to the regulation of the neuroinflammation in experimental autoimmune encephalomyelitis. J. Neuroimmunol 2007;191:16–25. [PubMed: 17904645]
36. van der Veen RC, Dietlin TA, Hofman FM, Pen L, Segal BH, Holland SM. Superoxide prevents nitric oxide-mediated suppression of helper T lymphocytes: decreased autoimmune encephalomyelitis in nicotinamide adenine dinucleotide phosphate oxidase knockout mice. J. Immunol 2000;164:5177–5183. [PubMed: 10799876]
37. Chu CQ, Wittmer S, Dalton DK. Failure to suppress the expansion of the activated CD4 T cell population in interferon γ-deficient mice leads to exacerbation of experimental autoimmune encephalomyelitis. J. Exp. Med 2000;192:123–128. [PubMed: 10880533]
38. van der Veen RC, Dietlin VTA, Hofman FM. Tissue expression of inducible nitric oxide synthase requires IFN-γ production by infiltrating splenic T cells: more evidence for immunosuppression by nitric oxide. J. Neuroimmunol 2003;145:86–90. [PubMed: 14644034]
39. Medzhitov R, Janeway CA Jr. Decoding the patterns of self and nonself by the innate immune system. Science 2002;296:298–300. [PubMed: 11951031]
40. Pasare C, Medzhitov R. Toll-like receptors and acquired immunity. Semin. Immunol 2004;16:23–26. [PubMed: 14751760]
41. Bronstein-Sitton N, Cohen-Daniel L, Vaknin I, Ezernitchi AV, Leshem B, Halabi A, Houri-Hadad Y, Greenbaum E, Zakay-Rones Z, Shapira L, Baniyash M. Sustained exposure to bacterial antigen induces interferon-γ-dependent T cell receptor ζ down-regulation and impaired T cell function. Nat. Immunol 2003;4:957–964. [PubMed: 14502285]
42. Ezernitchi AV, Vaknin I, Cohen-Daniel L, Levy O, Manaster E, Halabi A, Pikarsky E, Shapira L, Baniyash M. TCR ζ down-regulation under chronic inflammation is mediated by myeloid suppressor cells differentially distributed between various lymphatic organs. J. Immunol 2006;177:4763–4772. [PubMed: 16982917]
43. Reddy J, Waldner H, Zhang X, Illes Z, Wucherpfennig KW, Sobel RA, Kuchroo VK. Cutting edge: $CD4^+CD25^+$ regulatory T cells contribute to gender differences in susceptibility to experimental autoimmune encephalomyelitis. J. Immunol 2005;175:5591–5595. [PubMed: 16237044]
44. Korn T, Reddy J, Gao W, Bettelli E, Awasthi A, Petersen TR, Backstrom BT, Sobel RA, Wucherpfennig KW, Strom TB, et al. Myelin-specific regulatory T cells accumulate in the CNS but fail to control autoimmune inflammation. Nat. Med 2007;13:423–431. [PubMed: 17384649]

45. O'Connor RA, Malpass KH, Anderton SM. The inflamed central nervous system drives the activation and rapid proliferation of Foxp3 regulatory T cells. J. Immunol 2007;179:958–966. [PubMed: 17617587]

46. Sohrabji F. Guarding the blood-brain barrier: a role for estrogen in the etiology of neurodegenerative disease. Gene Expr 2007;13:311–319. [PubMed: 17708417]

47. Dietrich JB. Endothelial cells of the blood-brain barrier: a target for glucocorticoids and estrogens? Front Biosci 2004;9:684–693. [PubMed: 14766400]

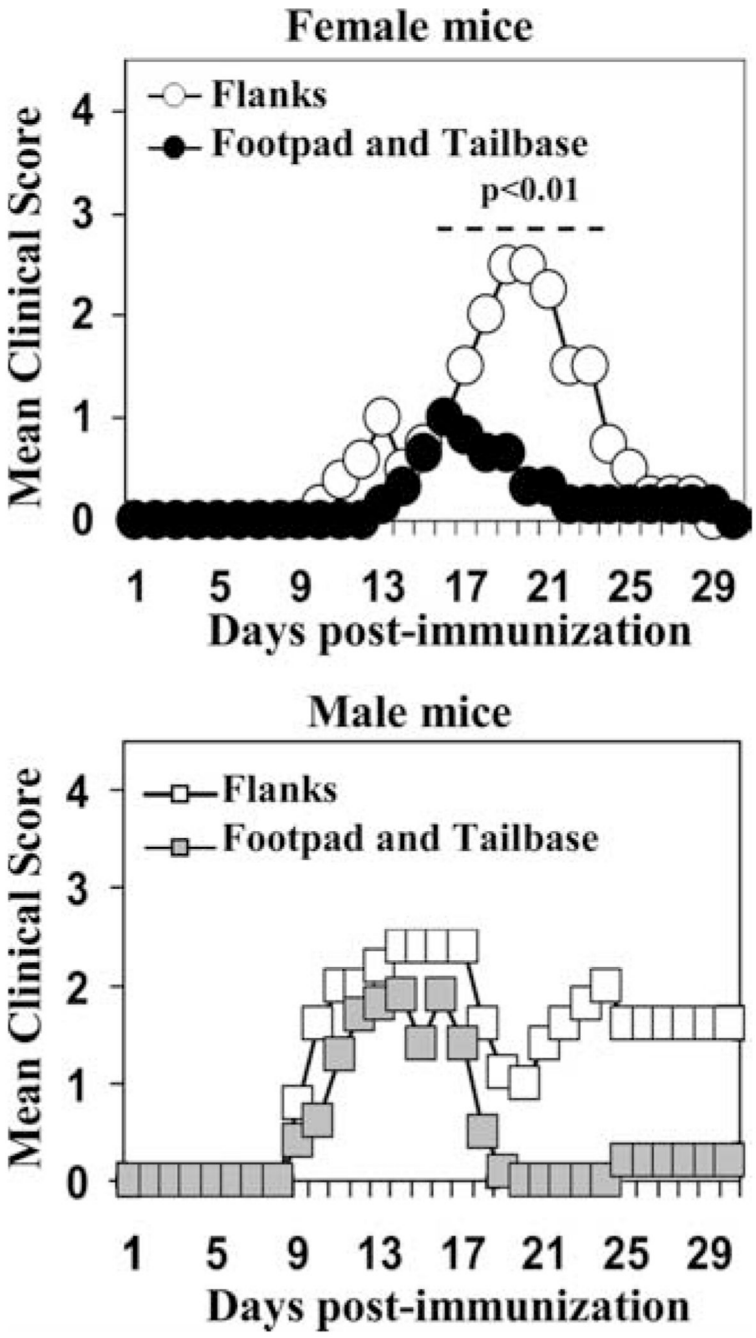

FIGURE 1.

Induction of EAE in male and female B10.PL following immunization with Ac1-9 peptide at different sites. Male and female mice (five mice per group) were immunized in the footpad/tailbase or in the flanks with 200 μg of the N-terminal-acetylated epitope of MBP, Ac1-9, emulsified in CFA supplemented with 4 mg/ml *Mycobacterium*. A total of 200 ng of pertussis toxin was i.p. administered on days 0 and 2 after immunization. The clinical score of EAE was determined daily as described in *Materials and Methods*. Disease incidence (number of mice showing disease symptoms/total number of mice) for each group was as follows: females, 2/5 mice (footpad/tailbase-immunized) and 4/5 mice (flank-immunized); males, 4/5 mice (footpad/tailbase-immunized) and 4/5 mice (flank-immunized). $p < 0.01$, significant differences

determined by Mann-Whitney *U* test were observed between female B10.PL mice immunized in the footpad/tailbase vs the flanks from days 17–23. No significant differences were found in male mice following immunization at different sites. Data are representative of at least four independent experiments.

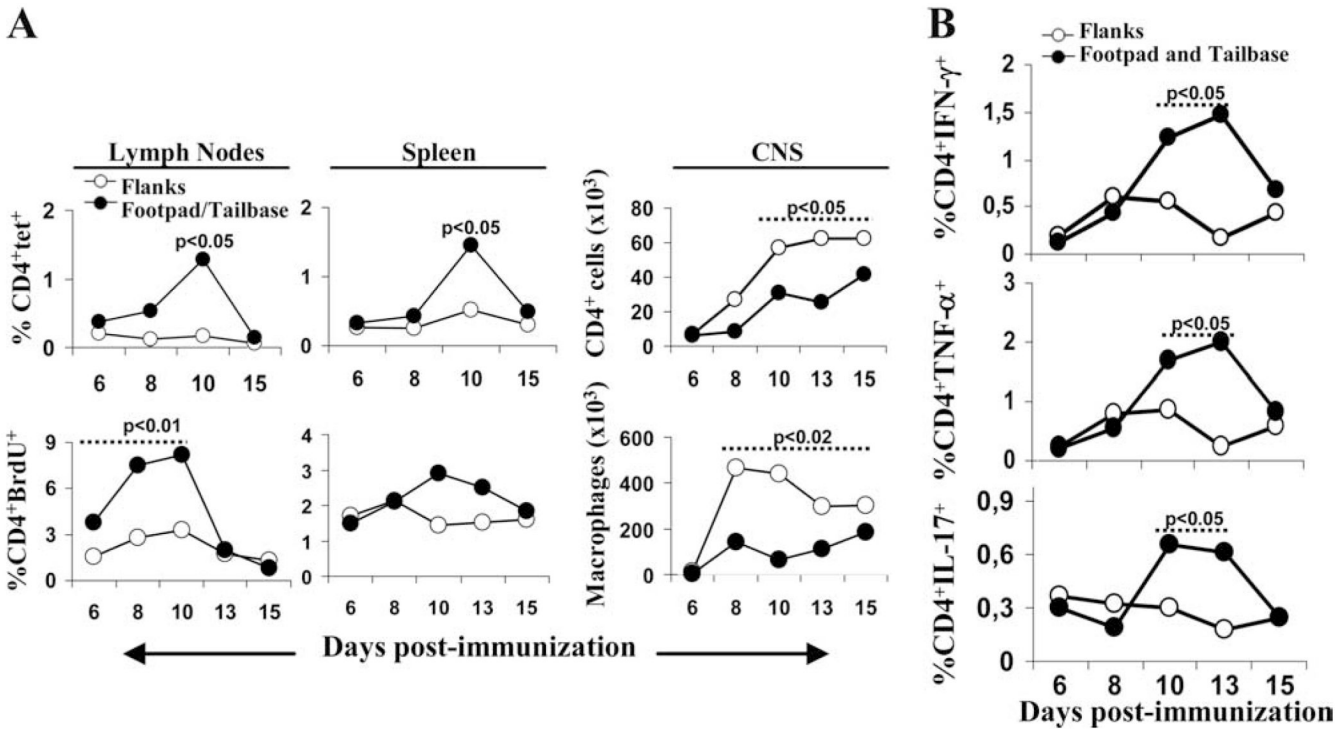

FIGURE 2.

Analyses of immune responses in female mice following immunization in the footpad and tailbase or flanks. Female B10.PL mice were immunized in the flanks or footpad/tailbase as described for Fig. 1. *A*, Percentage of Ag-specific tetramer-positive $CD4^+$ T cells ($CD4^+tet^+$) determined using PE-labeled MBP1-9[4Y]:I-A^u tetramers and PerCP-labeled anti-CD4 Abs in pooled (inguinal, popliteal, and cervical) LNs, spleens, and percentage of total $CD4^+$ T cells or macrophages in CNS samples, from mice at days 6, 8, 10, 13, and 15 after immunization. Samples were pooled from two mice per time point and treatment. In vivo proliferation of $CD4^+$ T cells was evaluated by i.p. injection of BrdU before harvesting LNs and spleens. Percentage of $CD4^+BrdU^+$ cells was determined by flow cytometry. *B*, Percentage of $CD4^+IFN\text{-}\gamma^+$-, $CD4^+TNF\text{-}\alpha^+$-, and $CD4^+IL\text{-}17^+$-producing T cells from mice following 6, 8, 10, 13, and 15 days immunization. Splenocytes were incubated with 10 μg/ml Ac1-9 for 4 h in the presence of Golgi Plug and cytokine production assessed by intracellular cytokine staining. Data in *B* show results from analyses of spleen cells pooled from two mice per time point and treatment. EAE scores of mice on day of sacrifice were 0, except for flank-immunized mice on day 10 (scores of 0 and 3), day 13 (scores of 0 and 1), and day 15 (scores of 0 and 2). Data are representative of at least two independent experiments. $p < 0.05$, $p < 0.02$, or $p < 0.01$ for significant differences determined by Mann-Whitney *U* test as indicated.

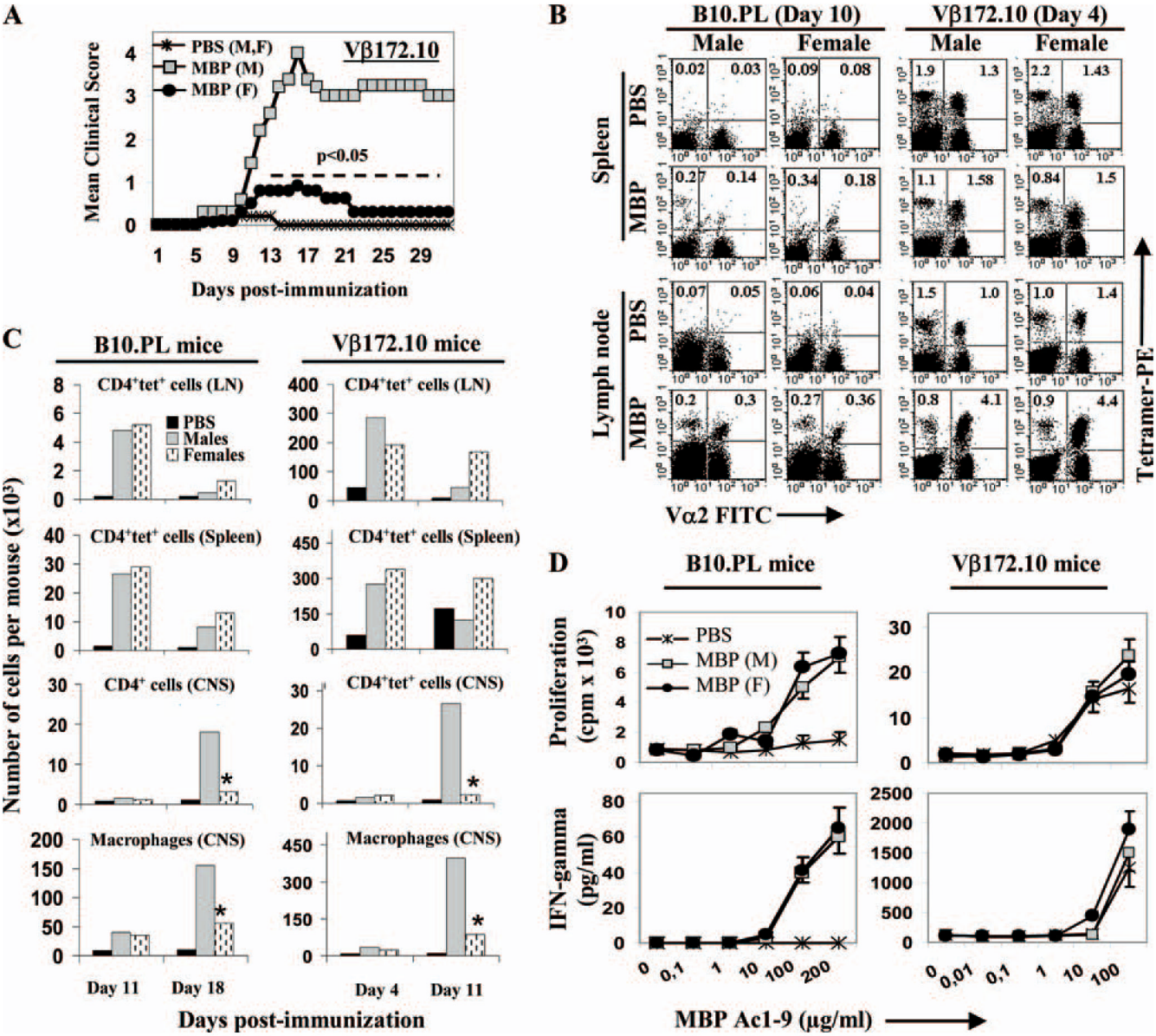

FIGURE 3.

EAE incidence and severity, absolute numbers and functional responses of Ag-specific T cells in male and female mice following footpad/tailbase immunization. Male or female B10.PL or Vβ172.10 mice were immunized with 200 μg of Ac1-9 in the footpad and tailbase, and B10.PL mice (but not Vβ172.10 mice) were treated with pertussis toxin as described for Fig. 1. *A*, Disease score in male (M) and female (F) Vβ172.10 mice. Disease incidence was 5/5 mice for males, and 2/5 for females. $p < 0.05$ for significant differences determined by Mann-Whitney *U* test observed between male and female Vβ172.10 mice from days 12–35. *B*, Analyses of a number of Ag-specific tetramer-positive $CD4^+$ T cells ($CD4^+tet^+$) using PE-labeled MBP1-9 [4Y]:I-A^u multimers/tetramers (5), FITC-labeled anti-Vα2, and PerCP-labeled anti-CD4 Abs following immunization of mice. Percentage of $CD4^+tet^+$ T cells ($V\alpha2^+$ or $V\alpha2^-$, as indicated in respective quadrants) in spleens and in pooled inguinal and popliteal LNs in male and female mice on day 10 (B10.PL mice) and day 4 (Vβ172.10 mice). Data in *B* show results from analyses of spleens or pooled inguinal and popliteal LNs from three mice per group. *C*, Number of cells

per mouse in spleens, LNs (inguinal and popliteal), and CNS following immunization. Data shown are derived from pooled organs from three mice per group. Mice were sacrificed on days 11 and 18 postim-munization for B10.PL mice and on days 4 and 11 postimmunization for Vβ172.10 mice. Analyses of the number of Ag-specific $CD4^+$ T cells were conducted using PE-labeled MBP1-9[4Y]:I-A^u tetramers (5,9), FITC-labeled anti-Vα2, PerCP-labeled anti-CD4, and allophycocyanin-labeled anti-CD45 Abs. Histogram plots represent the number of $CD4^+tet^+$ T cells or macrophages, except for CNS in B10.PL mice where the number of total $CD4^+$ T cells are shown due to the reduced number of $CD4^+tet^+$ T cells. *, $p < 0.05$ for significant differences determined by Mann-Whitneys *U* test between male and female mice. *D*, Proliferation and IFN-γ secretion of splenocytes isolated from male (M) and female (F) mice at day 11 postimmunization with Ac1-9 (MBP) following in vitro restimulation with Ac1-9. Cells were pooled from $n = 2$ to 3 mice per group. Error bars indicate SEs. Differences between male and female mice were not significant as determined by Kruskal-Wallis test. Data are representative of at least two independent experiments, with disease experiments (in *A*) being conducted three times.

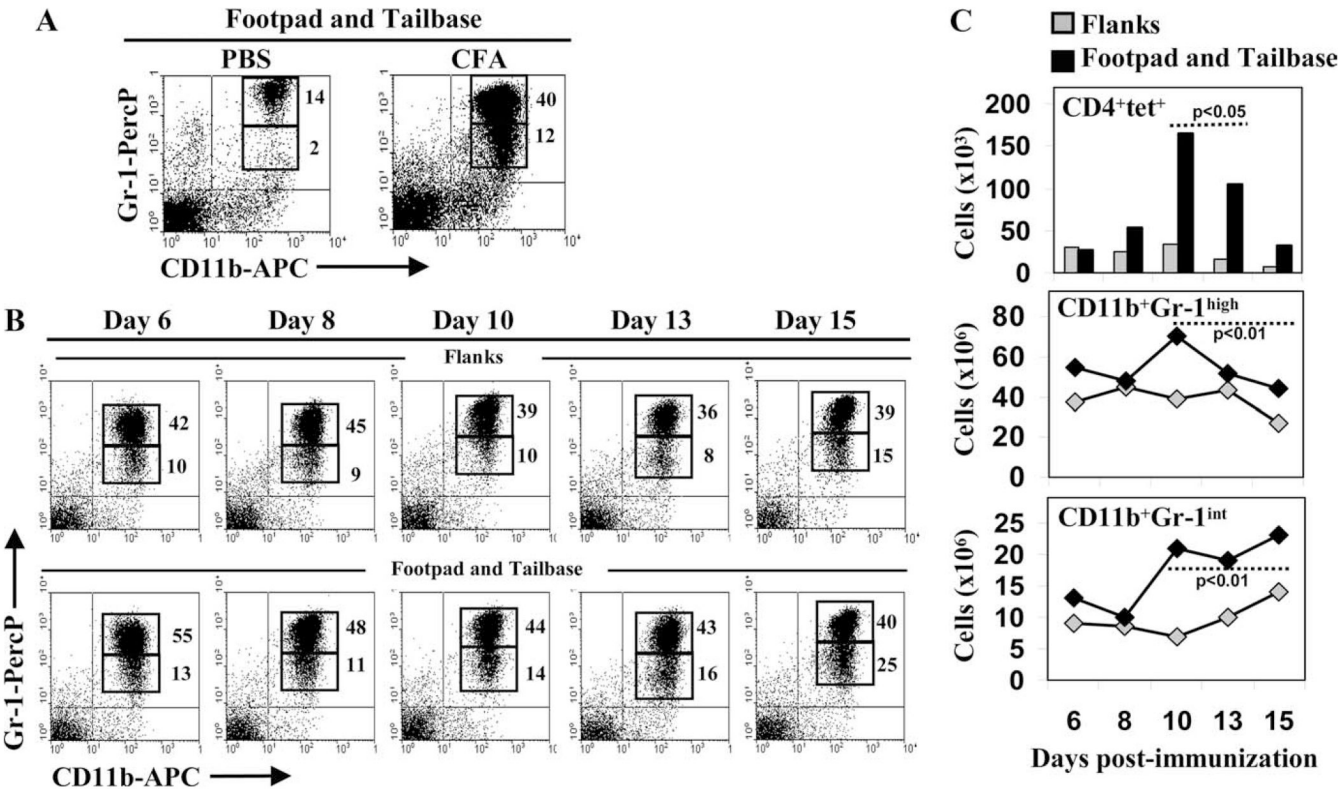

FIGURE 4.

Induction of myeloid cells following immunization of female B10.PL mice at different sites. *A*, Female mice were injected in the footpad with PBS or CFA and $CD11b^{+}Gr\text{-}1^{high}$ and $CD11b^{+}Gr\text{-}1^{int}$ myeloid cell populations analyzed by FSC/SSC and Gr1/CD11b parameters in pooled spleens 10 days later. Percentage of myeloid subsets in total splenocytes are shown. *B*, $Gr\text{-}1^{high}$ and $Gr\text{-}1^{int}$ myeloid cell populations in spleens were analyzed as in *A* for female mice immunized in footpad/tailbase or flanks (as described for Fig. 1) at different days postimmunization. *C*, Absolute numbers of Ag-specific tetramer-positive $CD4^{+}$ T cells ($CD4^{+}tet^{+}$), $CD11b^{+}Gr\text{-}1^{high}$, and $CD11b^{+}Gr\text{-}1^{int}$ myeloid cells for the same animals that were used to generate data shown in *B*. Data in *A* and *C* show results from analyses of organs pooled from two mice per group. For *B* and *C*, EAE scores of mice on day of sacrifice were 0, except for flank-immunized mice on day 10 (scores of 0 and 3), day 13 (scores of 0 and 1), and day 15 (scores of 0 and 2). $p < 0.05$ or $p < 0.01$ for significant differences determined by Mann-Whitney *U* test between flank- and footpad/tailbase-immunized mice. Data are representative of at least two independent experiments.

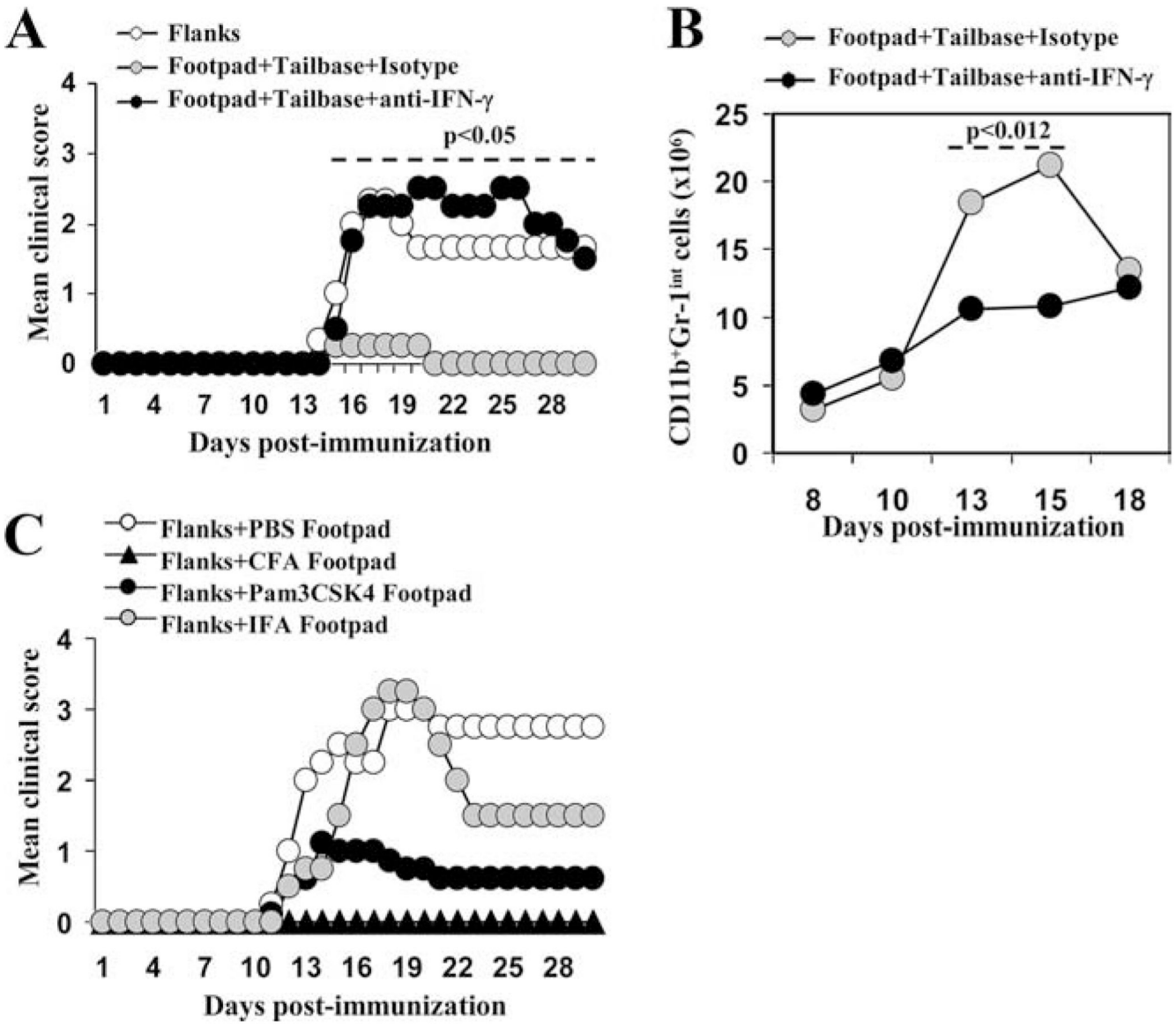

FIGURE 5.

Impact of IFN-γ blockade and adjuvants on EAE induction in female mice. *A*, Female B10.PL mice (five mice per group) were immunized in the flanks (control group), or in the footpad/tailbase with 200 μg of Ac1-9 emulsified in CFA. Pertussis toxin was delivered i.p. on days 0 and 2 postimmunization (200 ng). Mice immunized in the footpad/tailbase were treated with 100 μg of anti-IFN-γ Ab, or isotype-matched control Ab, on days 6 and 9 postimmunization. Both flank-immunized mice and mice immunized in the footpad/tailbase followed by treatment with anti-IFN-γ Ab showed significantly higher EAE scores relative to footpad/tailbase-immunized mice treated with isotype control. $p < 0.05$ by Mann-Whitney *U* test for days 16–30. No significant difference between flank-immunized mice and footpad/tailbase-immunized mice treated with anti-IFN-γ Ab was found. *B*, Analysis of the number of $CD11b^{+}Gr1^{int}$ cells in spleens of female B10.PL mice following treatment of mice as in *A*. Data shown represent mean cell number for individual spleens isolated from a total of $n = 4–7$ mice for each time point shown, and are compiled from three different experiments. Mice treated with anti-IFN-γ Ab show a significantly lower number of $CD11b^{+}Gr1^{int}$ cells in spleens relative to isotype

control treated mice on days 13 and 15. $p = 0.012$ by Mann-Whitney *U* test. *C*, Female B10.PL mice (five mice per group) were injected in the footpad with PBS, CFA, Pam_3CSK_4, or IFA, immediately following immunization with Ac1-9 in the flanks. Mice treated in the footpad with CFA showed lower clinical scores relative to animals treated with PBS or IFA. $p < 0.05$ for comparison with PBS for days 14–21 or $p < 0.05$ for comparison with IFA for days 17–19 determined by Mann-Whitney *U* test. No significant difference was found when CFA and Pam_3CSK_4 treatments were compared. Data shown are representative of at least two independent experiments.